

Description of gradient-index crystalline lens by a first-order optical system

M V Pérez, C Bao, M T Flores-Arias, M A Rama and C Gómez-Reino

GRIN Optics Group¹, Department of Applied Physics, Faculty of Physics and Optics and Optometry School, Campus Sur, University of Santiago de Compostela, E15782 Santiago de Compostela, Spain

E-mail: facgre@usc.es (C Gómez-Reino)

Received 29 November 2004, accepted for publication 22 December 2004

Published 11 January 2005

Online at stacks.iop.org/JOptA/7/103

Abstract

This paper uses the correspondence between the canonical integral transform and the ray-transfer matrix of a first-order optical system to analyse paraxial properties of the crystalline lens of the human eye regarded as a gradient-index (GRIN) medium limited by curved surfaces. Matrix factorization is provided to evaluate cardinal elements and refractive powers of the crystalline lens.

Keywords: crystalline lens, GRIN optics, first-order systems

1. Introduction

A first-order or $ABCD$ optical system is a weakly inhomogeneous (GRIN) medium with quadratic transversal refractive index [1]. This definition includes, as particular cases, a number of relevant discrete optical elements such as lenses, mirrors, etc, as well as optical systems with constant refractive index. The propagation of light through a first-order optical system is described in the paraxial (or parabolic) approximation by a linear integral transform called the canonical integral (or generalized Fresnel) transform. This transform

$$F(x; z) = \int_{-\infty}^{\infty} f(x_0) K(x_0, x; z) dx_0 \quad (1)$$

for a 1D system, with the kernel

$$K(x_0, x; z) = \begin{cases} \frac{1}{\sqrt{i2\pi B}} \exp\left\{ik \frac{Ax_0^2 + Dx^2 - 2xx_0}{2B}\right\} & B \neq 0 \\ \frac{1}{\sqrt{A}} \exp\left\{ik \frac{Cx^2}{2A}\right\} \delta\left(x_0 - \frac{x}{A}\right) & B = 0 \end{cases} \quad (2)$$

has been known in optics for a long time [2–4] and has been applied for a self-contained mathematical description of the field evolution in first-order optical systems. Its kernel is

¹ <http://www.usc.es/grinteam>

expressed through the elements of the ray-transfer $ABCD$ matrix relating the positions x_0, x and the slopes \dot{x}_0, \dot{x} of the ray at two transversal planes along the z propagation direction.

$$\begin{pmatrix} x \\ \dot{x} \end{pmatrix} = \begin{pmatrix} A & B \\ C & D \end{pmatrix} \begin{pmatrix} x_0 \\ \dot{x}_0 \end{pmatrix} \quad (3)$$

the dot being the derivative with respect to z .

The connection between (2) and (3) leads to useful relations between geometrical ray optics and the operator representation of wave optics [5–10]. So, the great interest of the first-order optical systems is their potentiality to analyse light propagation by using either matrix algebra or operator algebra, whichever is more convenient. The Fresnel and Fourier transforms are particular cases of the canonical integral transform which adequately describe the diffraction of the light in first-order systems. They correspond to the canonical integral transform parametrized by particular values of the elements of the ray-transfer matrix. This matrix is a linear transformation which expresses the ray trajectory in a first-order system and which permits us to evaluate paraxial properties of such a system.

On the other hand, the refractive index of the crystalline lens is not constant and the lens can be regarded as a GRIN structure, in the paraxial approximation, with quadratic transversal refractive index modulated by an axial index which is given, in the sagittal section of the lens, by

$$n(x, z) = n_0(z) \left[1 - \frac{g^2(z)}{2} x^2 \right] \quad (4)$$

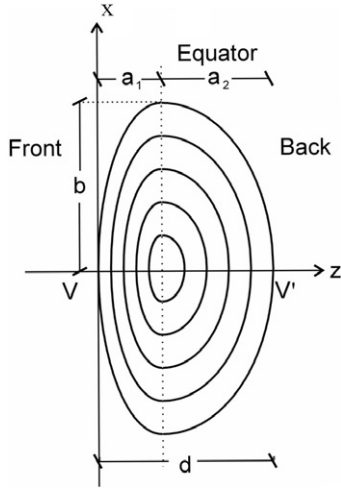


Figure 1. Refractive index distribution of the crystalline lens in the sagittal section represented as bi-elliptical iso-indicial curves joined at the equator. For the iso-indicial curves the origin of the axis is at the front vertex V.

where $n_0(z)$ is the refractive index along the z axis and $g(z)$ is the gradient parameter describing the evolution of the transverse parabolic distribution.

The expressions for n_0 and g depend on the optical modelling of inhomogeneity of the refractive index within the lens. For the continuous GRIN model, the refractive index profile is represented by continuous iso-indicial surfaces of different shapes [11–16]. In particular, for the asymmetric bi-elliptical model that provides a close simulation to the real situation, n_0 and g can be written as [17]

$$g_f^2(z) = -\frac{\sum_{j=1}^{\infty} 2j c_j \left[\frac{z-a_1}{a_1} \right]^{2(j-1)}}{b^2 n_{0f}(z)} \quad (5)$$

$$n_{0f}(z) = n_f(x, z)|_{x=0} = \sum_{j=0}^{\infty} c_j \left(\frac{z-a_1}{a_1} \right)^{2j} \quad (6)$$

for the front part of the lens and

$$g_b^2(z) = -\frac{\sum_{j=1}^{\infty} 2j c_j \left[\frac{z-a_1}{a_2} \right]^{2(j-1)}}{b^2 n_{0b}(z)} \quad (7)$$

$$n_{0b}(z) = n_b(x, z)|_{x=0} = \sum_{j=0}^{\infty} c_j \left(\frac{z-a_1}{a_2} \right)^{2j} \quad (8)$$

for the back part of the lens, where subscripts f and b denote front and back parts of the lens, c_j are coefficients of the power series, b is the common semi-axis of ellipses along the z -axis and a_1 and a_2 are the semi-axes along the z -axis of the asymmetric bi-elliptical iso-indicial curves (see figure 1).

So, as mentioned above, the crystalline lens operating in the paraxial regime with refractive index given by equation (4) is referred to as a first-order system or *ABCD* one. The ray-transfer matrix is expressed in the GRIN crystalline lens by [1, 18]

$$M(z) = \begin{pmatrix} H_f(z) & H_a(z) \\ \dot{H}_f(z) & \dot{H}_a(z) \end{pmatrix} \quad (9)$$

whose determinant is equal to unity and which describes the ray transformation in such a lens.

$\overset{(\cdot)}{H}_f$ and $\overset{(\cdot)}{H}_a$ are the position and the slope of the field and axial rays at plane z . They univocally determine the elements which define the matrix $M(z)$ and they were introduced by Luneburg to facilitate the analysis of paraxial light propagation in GRIN media [1].

The main line of this paper is to describe analytically light propagation through a first-order optical system based on the correspondence between the canonical integral transform and its ray-transfer matrix and to discuss its use for the analysis of paraxial properties of the crystalline lens. The correspondence permits us to decompose the transform as the product of three linear operators associated with three basic matrices having a simple geometrical meaning. This matrix factorization can be easily used to evaluate the cardinal elements and refractive power of the lens. In this way the *ABCD* matrix becomes a powerful and synthetic tool for understanding properties of the light beams in the passage through the crystalline lens as a first-order system.

2. Paraxial properties of the crystalline lens: decomposition of the *ABCD* matrix

The optical properties of the crystalline lens are dependent on the curvature radii of the front and back surfaces and the variation of the refractive index within the lens due to its GRIN nature. The light propagation through the whole lens combines discrete refraction at the end surfaces with continuous refraction within it. In order to make a detailed analysis of these properties we will use the ray-transfer matrix that represents the action of the lens on the light propagation in the paraxial regime.

2.1. Matrix of the crystalline lens

If we consider a lens of thickness d ($=a_1 + a_2$) along the z axis, the ray-transfer matrix can be expressed as the following multiplication of matrices:

$$\begin{pmatrix} 1 & 0 \\ -P_b/n'_1 & n_e/n'_1 \end{pmatrix} \begin{pmatrix} H_f(d) & H_a(d) \\ \dot{H}_f(d) & \dot{H}_a(d) \end{pmatrix} \begin{pmatrix} 1 & 0 \\ -P_f/n_e & n_1/n_e \end{pmatrix} \quad (10)$$

where the first and third matrices are the refraction matrices at the back and front surfaces of the whole lens and the second one is the ray-transfer matrix, given by equation (9), corresponding to the light propagation through the GRIN crystalline of thickness d . P_f and P_b are the powers of the front and back surfaces, n_1 and n'_1 are the indices before and behind the lens, and n_e is the index at the edge of the lens (figure 2). Likewise, $\overset{(\cdot)}{H}_f(d)$ and $\overset{(\cdot)}{H}_a(d)$ are the position and the slope of the field and axial ray at d , given by [17]

$$H_a(d) = d \left(1 - \frac{g_c^2 d^2}{6} \right) \quad (11)$$

$$\begin{aligned} H_f(d) &= 1 - \frac{g_c^2 d^2}{2} + \frac{\dot{g}_c d}{2g_c} \left(1 - \frac{g_c^2 d^2}{6} \right) \\ &= 1 - \frac{g_c^2 d^2}{2} + \frac{\dot{g}_c}{2g_c} H_{ab}(d) \end{aligned} \quad (12)$$

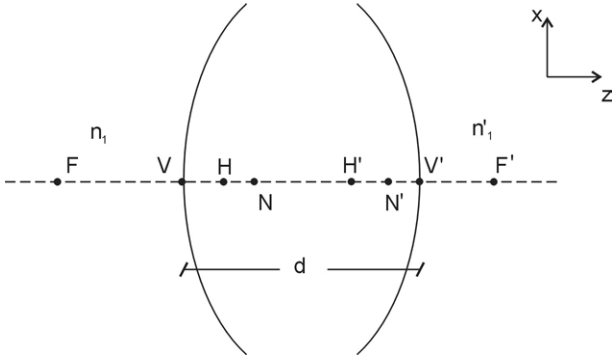


Figure 2. Crystalline lens as a GRIN lens limited by curved surfaces: cardinal elements.

$$\begin{aligned} \dot{H}_a(d) &= 1 - \frac{g_e^2 d^2}{2} - \frac{\dot{g}_e d}{2g_e} \left(1 - \frac{g_e^2 d^2}{6}\right) \\ &= 1 - \frac{g_e^2 d^2}{2} - \frac{\dot{g}_e}{2g_e} H_{ab}(d) \end{aligned} \quad (13)$$

$$\begin{aligned} \dot{H}_f(d) &= -g_e d \left(1 - \frac{g_e^2 d^2}{6}\right) \left(g_e + \frac{\dot{g}_e}{4g_e^3}\right) \\ &= -\left(g_e^2 + \left(\frac{\dot{g}_e}{2g_e}\right)^2\right) H_{ab}(d). \end{aligned} \quad (14)$$

In the above equations, the relationship between the slope \dot{g}_e of the gradient parameter and this parameter g_e at d can be written as

$$\frac{\dot{g}_e}{2g_e} = -\frac{n_c \sum_{j=2}^{\infty} j(j-1)c_j - [\sum_{j=1}^{\infty} j c_j]^2}{2dn_c \sum_{j=1}^{\infty} j c_j} \quad (15)$$

with

$$g_e^2 = -\frac{2 \sum_{j=1}^{\infty} j c_j}{b^2 n_c}. \quad (16)$$

Performing the matrix multiplication, one gets for the crystalline lens that

$$\begin{pmatrix} H_f(d) - \frac{P_f H_a(d)}{n_e} \\ -\frac{1}{n'_1} \left[P_b H_f(d) - \frac{P_b P_f H_a(d)}{n_e} + P_G + P_f \dot{H}_a(d) \right] \\ \frac{n_1}{n'_1} H_a(d) \\ \frac{n_1}{n'_1} \left[\dot{H}_a(d) - \frac{P_b H_a(d)}{n_e} \right] \end{pmatrix} = \begin{pmatrix} A & B \\ C & D \end{pmatrix} \quad (17)$$

such that

$$AD - BC = n_1/n'_1 \quad (18)$$

where Lagrange's invariant

$$H_f(d)\dot{H}_a(d) - \dot{H}_f(d)H_a(d) = 1 \quad (19)$$

has been used and P_G is the refractive power of the lens due only to its GRIN nature expressed as [17]

$$P_G = -n_c \dot{H}_f(d). \quad (20)$$

2.2. Decomposition of the ABCD matrix: cardinal elements and power of the crystalline lens

The correspondence between the canonical integral transform and its transfer matrix, given by equation (17), permits us

to decompose the transform as the product of three linear operations associated with three basic matrices having a simple geometrical meaning. This matrix factorization is written [19]

$$\begin{pmatrix} A & B \\ C & D \end{pmatrix} = \begin{pmatrix} 1 & 0 \\ C/A & 1 \end{pmatrix} \begin{pmatrix} A & 0 \\ 0 & 1/A \end{pmatrix} \begin{pmatrix} 1 & B/A \\ 0 & 1 \end{pmatrix} \quad (21)$$

for $A \neq 0$.

The decomposition of the ray-transfer matrix can be interpreted as the passage of the light through three simpler cascaded systems. The first matrix represents the passage through a lens of focal length $-A/C$, measured from the back face of the lens. The second one is associated with a transverse magnification by a factor A (change of variable $x \rightarrow x/A$). The third one is a free propagation to a distance B/A . From the first matrix we have that the back vertex focal length is given by

$$\begin{aligned} V'F' &= -A/C \\ &= \frac{n'_1 [n_e H_f(d) - P_f H_a(d)]}{n_e [P_b H_f(d) + P_f \dot{H}_a(d) + P_G] - P_b P_f H_a(d)}. \end{aligned} \quad (22)$$

From the second matrix we obtain the transverse magnification

$$M_t = A = H_f(d) - \frac{P_f H_a(d)}{n_e}. \quad (23)$$

The back focal length measured from the back principal point H' can be found by taking into account that the principal planes have unit positive transverse magnification. Therefore, we can use the condition $M_t = 1$ to get the back focal distance

$$\begin{aligned} H'H' &= -1/C \\ &= \frac{n'_1 n_e}{n_e [P_b H_f(d) + P_f \dot{H}_a(d) + P_G] - P_b P_f H_a(d)}. \end{aligned} \quad (24)$$

The distance from the back vertex to the back principal point can be known if we use equations (22) and (23) and it is given by

$$\begin{aligned} V'H' &= \frac{1-A}{C} \\ &= \frac{n'_1 [n_e (H_f(d) - 1) - P_f H_a(d)]}{n_e [P_b H_f(d) + P_f \dot{H}_a(d) + P_G] - P_b P_f H_a(d)}. \end{aligned} \quad (25)$$

It is worthwhile to emphasize the quantitative information contained in the factorization of the ABCD matrix. In this way, the back vertex power of the lens is expressed as

$$\begin{aligned} P_{V'} &= \frac{n'_1}{V'F'} = -\frac{n'_1 C}{A} \\ &= \frac{n_e [P_b H_f(d) + P_f \dot{H}_a(d) + P_G] - P_b P_f H_a(d)}{n_e H_f(d) - P_f H_a(d)} \end{aligned} \quad (26)$$

and the back refractive power or equivalent power is written as

$$\begin{aligned} P_E &= \frac{n'_1}{H'F'} = -n'_1 C \\ &= P_b H_f(d) + P_f \dot{H}_a(d) + P_G - \frac{P_b P_f H_a(d)}{n_e}. \end{aligned} \quad (27)$$

Note that equation (27) becomes the well known equivalent power equation for a homogeneous thick lens of refractive index n_e and thickness d in which $H_f(d) = \dot{H}_a(d) = 1$, $H_a(d) = d$ and $P_G = 0$.

The above equation can be rewritten, in terms of the distance d_f from the front surface to the front principal point and the distance d_b from the back principal point to the back surface due to only the GRIN nature of the lens, as (see the appendix)

$$P_E = P_f + P_b + P_G - \frac{d_b}{n'_1} P_b P_G - \frac{d_f}{n_1} P_f P_G - \left(\frac{d_f}{n_1} + \frac{d_b}{n'_1} \right) P_b P_f + \frac{d_f d_b}{n_1 n'_1} P_b P_f P_G \quad (28)$$

which is probably the equivalent power equation of an optical system formed by three thin lenses [20].

Finally, the third matrix of factorization represents a free propagation to a equivalent distance

$$l'_{eq} = B/A = \frac{n_1 H_a(d)}{n_e H_f(d) - P_f H_a(d)}. \quad (29)$$

On the other hand, the position of the remaining back cardinal point, that is, the back nodal point, is expressed as [5]

$$V'N' = -\frac{1}{C} \left(A - \frac{n_1}{n'_1} \right) = \frac{n'_1 [n_e H_f(d) - P_f H_a(d)] - n_e n_1}{n_e P_E} \quad (30)$$

where equations (17) and (27) have been used.

From equations (25) and (30) it follows that the separation between back principal and nodal points is given by

$$H'N' = \frac{n_1 - n'_1}{P_E}. \quad (31)$$

Therefore, equation (25) reduces to equation (30) and principal and nodal points coincide as $n_1 = n'_1$.

The number of possible decompositions of the $ABCD$ matrix in terms of propagation, magnification and passage through a lens is the same as the six permutations of the above transformations. This fact permits us to obtain the cardinal elements and power referred to the front part of the system. So, we now write the factorization as

$$\begin{pmatrix} A & B \\ C & D \end{pmatrix} = \begin{pmatrix} 1 & B/D \\ 0 & 1 \end{pmatrix} \begin{pmatrix} 1/D & 0 \\ 0 & D \end{pmatrix} \begin{pmatrix} 1 & 0 \\ C/D & 1 \end{pmatrix} \quad (32)$$

for $D \neq 0$.

The factorization given by equation (32) appears in inverse order to that given by equation (21). Note that the first matrix represents a free propagation to a distance B/D , the second one indicates an angular magnification by a factor D (change of variable $\dot{x} \rightarrow \dot{x}/D$) and the third one is associated with the passage of light through a lens of focal length D/C measured from the front face of the lens.

The second and third matrices of equation (32) carry information on the positions of the front cardinal points which are written for the crystalline lens as

$$VF = \frac{D}{C} - \frac{n_1 [n_e \dot{H}_a(d) - P_b H_a(d)]}{n_e P_E} \quad (33)$$

$$VN = \frac{D-1}{C} = \frac{n_e n'_1 - n_1 [n_e \dot{H}_a(d) - P_b H_a(d)]}{n_e P_E} \quad (34)$$

$$VH = \frac{1}{C} \left(D - \frac{n_1}{n'_1} \right) = -\frac{n_1 [n_e (\dot{H}_a(d) - 1) - P_b H_a(d)]}{n_e P_E}. \quad (35)$$

The front focal length can be found if we use equations (33) and (35), that is

$$HF = \frac{n_1}{n'_1 C} = -\frac{n_1}{P_E} \quad (36)$$

where equation (27) has been used.

Likewise, the front vertex power is given by

$$P_V = -\frac{n_1}{VF} = -\frac{n_1 C}{D} = \frac{n_e P_E}{n_e \dot{H}_a(d) - P_b H_a(d)} \quad (37)$$

where equation (33) has been used.

The spacing between the principal points can be written as (see figure 2)

$$t = HH' = d - \{n_1 [P_b H_a(d) - n_e (\dot{H}_a(d) - 1)] + n'_1 [P_f H_a(d) - n_e (H_f(d) - 1)]\} \{n_e P_E\}^{-1} \quad (38)$$

where equations (25) and (35) have been used.

Similarly, from equations (30) and (34), the spacing between nodal points is expressed as

$$e = NN' = d - \{n_1 [P_b H_a(d) - n_e (\dot{H}_a(d) - 1)] + n'_1 [P_f H_a(d) - n_e (H_f(d) - 1)]\} \{n_e P_E\}^{-1}. \quad (39)$$

We obtain a well known result in first-order systems that says that the distance between the nodal points is equal to the distance between the principal points and when $n_1 = n'_1$ the nodal and the principal points coincide.

Finally, the first matrix represents free propagation through an equivalent distance given by

$$l_{eq} = \frac{B}{D} = \frac{n_1 H_a(d)}{n_e H_a(d) - P_b H_a(d)} \quad (40)$$

where equation (17) has been used.

3. Results

In order to analyse the paraxial properties of the crystalline lens from its GRIN nature and curved surfaces, we have considered a lens characterized by a transversal parabolic refractive index distribution, given by equation (4), modulated by a longitudinal refractive index along the z optical axis containing up to a sixth order in z . Values of central refractive index of 1.406 and edge index of 1.386 were taken from the Gullstrans schematic eye [21]. The coefficients c_j of the power series in the refractive index profile were found by the weak inhomogeneity condition [17, 18]. Changes with age in thickness and radii of curvature of surfaces of the lens for unaccommodated eyes were taken from studies of Koretz and co-workers [22, 23]. Figure 3 depicts equivalent power versus thickness and equatorial radius of the crystalline lens. A quasi-linear increase of the equivalent power with thickness is shown in figure 3(a) for an equatorial radius of 4.5 mm and for different numbers of coefficients in the refractive index. The equivalent power is higher for two coefficients than for three and four coefficients in the refractive index. At the last two cases, the equivalent power achieves almost the same value. Lens refractive power varies by almost 4 D around a value of 19.5 D achieved for a lens thickness of 4.1 mm. Figure 3(b) represents the equivalent power versus equatorial radius for a lens thickness of 4 mm and for different numbers of coefficients

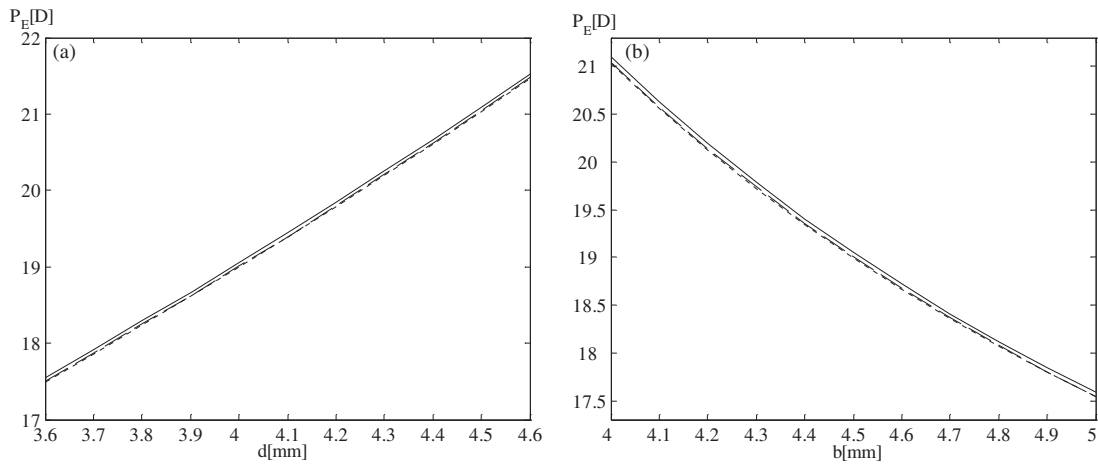


Figure 3. Equivalent power versus (a) thickness and (b) equatorial radius. Calculations have been made for $c_0 = 1.406$ and $c_1 = -0.02$ (solid curve), $c_1 = -0.0201$ and $c_2 = 0.0001$ (dashed curve) and $c_1 = -0.0201416$, $c_2 = 0.0001423$ and $c_3 = -0.0000007$ (dotted curve). For (a) $b = 4.5$ mm and for (b) $d = 4$ mm.

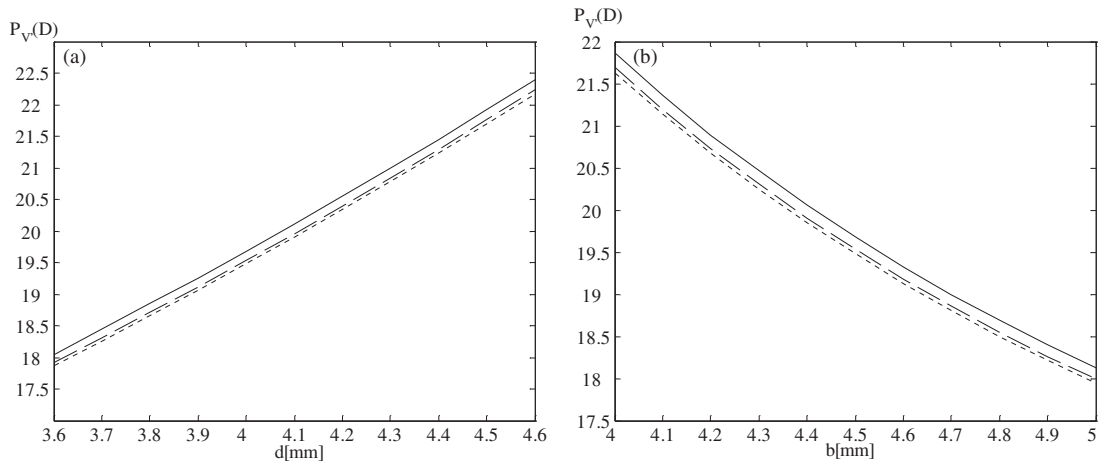


Figure 4. Back refractive power versus (a) thickness and (b) equatorial radius. Calculations have been made for values of figure 3.

in the refractive index. A decrease of almost 3.5 D in the refractive power can be observed instead of an increase as in figure 3(a). The equivalent power is higher for two coefficients than for three and four coefficients, having almost the same behaviour for the highest orders of the refractive index along the optical axis. Figure 4 represents the back vertex power versus thickness and equatorial radius of the lens. A similar behaviour to that in figure 3 can be observed. However, a difference in power of 0.5 D between the lowest order and the highest orders of the refractive index is achieved, being higher than that obtained for equivalent power. Likewise, power values for four coefficients in the refractive index are lower than for two and three coefficients.

Figure 5 depicts the variation of the front vertex power with thickness and equatorial radius of the crystalline lens. A quasi-linear increase and a non-linear decrease of the front vertex power occur with thickness (figure 5(a)) and equatorial radius (figure 5(b)), respectively, as in figure 4. In contrast, the front vertex power for four and three coefficients in the refractive index is higher than for two coefficients.

Figures 6 and 7 represent the position of the cardinal points of the crystalline lens, measured from vertices, versus d and

b for $n_1 = n'_1$ (nodal and principal points coincide) and for different numbers of coefficients in the refractive index along the z optical axis. Figures 6(a) and (d) depict the position of the back principal point versus thickness and equatorial radius, and figures 6(c) and (d) show the variation of position of the back focal point with these parameters. The back principal point is located on the left of the back vertex and inside the lens as shown in figures 6(a) and (b). It moves away from the vertex as thickness increases for all cases. The shift from the vertex is higher for two coefficients than for three and four (figure 6(a)). However, the position moves back to the vertex slowly with b for four coefficients, it is almost constant for three coefficients and it moves away from the vertex for two coefficients as occurs in figure 6(b). The back focus is on the right of the back vertex and it moves back to the vertex as the thickness increases (figure 6(c)). It has a reverse behaviour with equatorial radius (figure 6(d)). In both cases, the distances from the vertex to the focus are higher for four and three coefficients than for two coefficients. Figures 7(a) and (b) depict the variation of the position of the front principal point with thickness and equatorial radius and figures 7(c) and (d) represent the position of the front focal point versus both

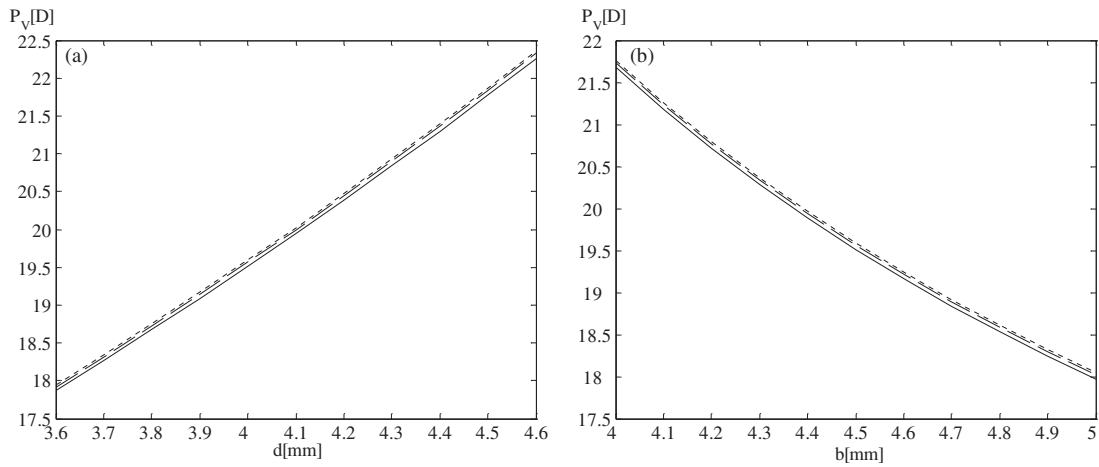


Figure 5. Front refractive power versus (a) thickness and (b) equatorial radius. Calculations have been made for values of figure 3.

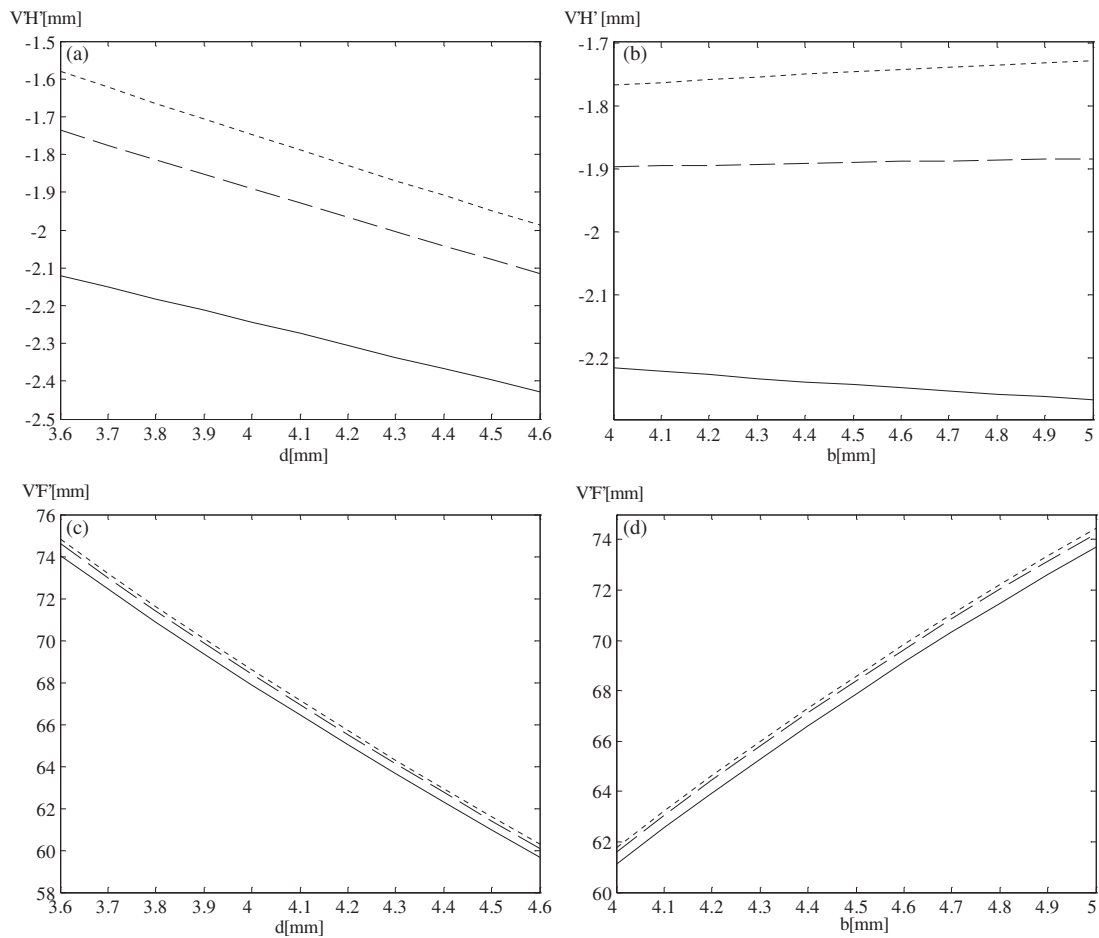


Figure 6. Position of the back principal point versus thickness (a) and equatorial radius (b) and position of the back focal point versus thickness (c) and equatorial radius (d). Calculations have been made for values of figure 3.

parameters. The front principal point is located on the right of the front vertex and inside the lens as shown in figures 7(a) and (b). A similar behaviour for the position variation of the front principal point to that in figures 6(a) and (b) occurs. The front focus is located on the left of the front vertex and it moves back to the front vertex as the thickness increases (figure 7(c)) and moves away from the front vertex as the equatorial radius

increases (figure 7(d)). In both cases, a very weak dependence on the number of coefficients is shown. Finally, the variation of the separation between principal points with thickness is represented in figure 8. The spacing between the principal points remains almost constant for the three cases. In a precise manner, the separation increases slightly with thickness up to values around 4.3 mm and a decrease occurs from this value.

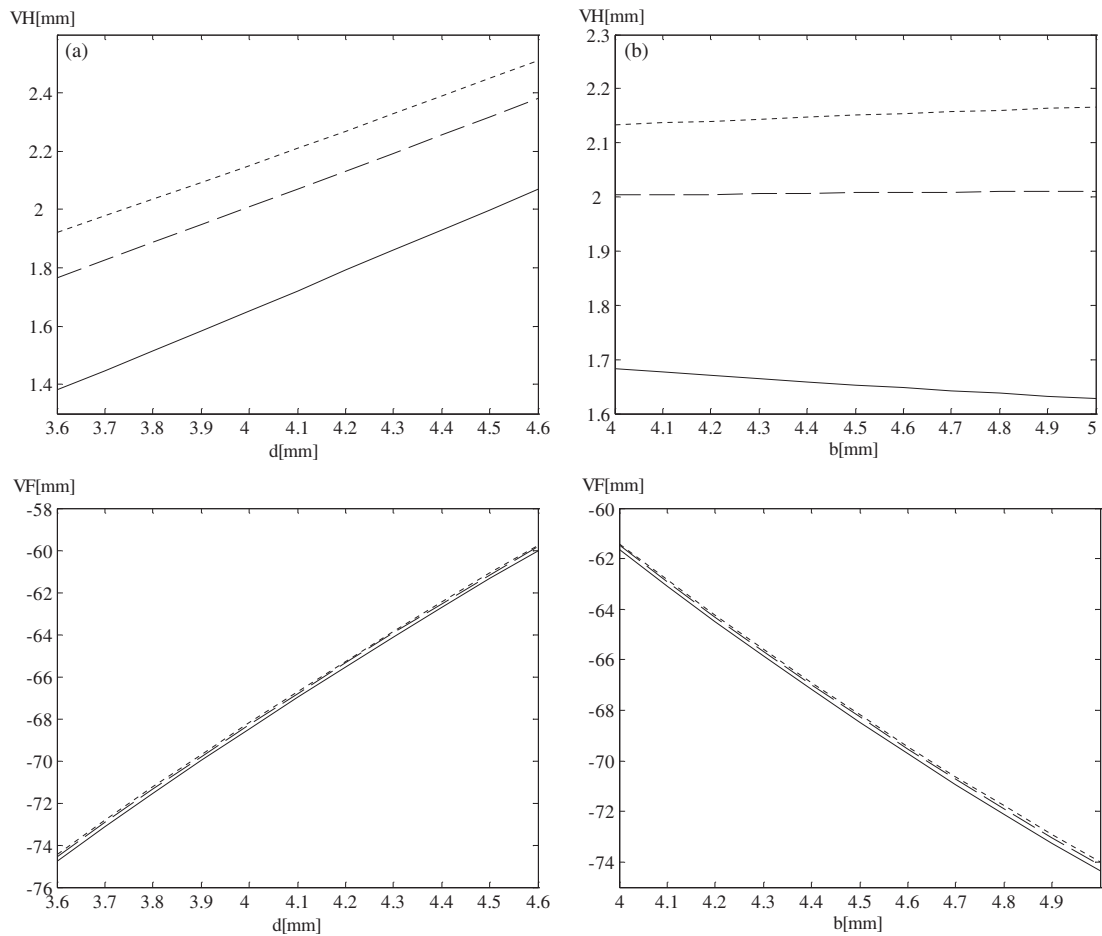


Figure 7. Position of the front principal point versus thickness (a) and equatorial radius (b) and position of the front focal point versus thickness (c) and equatorial radius (d). Calculations have been made for values of figure 3.

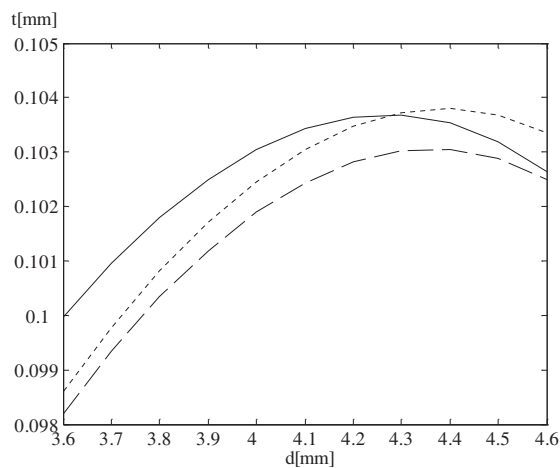


Figure 8. Separation between principal points versus thickness. Calculations have been made for values of figure 3.

The spacing for three coefficients is lower than for four and two coefficients in the refractive index along the axis.

4. Conclusions

Using the correspondence between the canonical integral transform and the ray-transfer matrix of the crystalline lens

as a first-order optical system, we have presented, in an easy manner, analytical expressions for evaluating the paraxial properties of the human lens regarded as a GRIN medium limited by curved surfaces. In particular, the cardinal element location and refractive powers of the crystalline lens, with transversal refractive index distribution modulated by a longitudinal refractive index along the z optical axis containing up to a sixth order in z , have been calculated in terms of the elements of the ray-transfer matrix that describe light propagation through first-order systems. Results show that the paraxial properties of the lens are sensitive to the form of the axial refractive index profile, specially for two coefficients. The sensitive decreases as the number of coefficients in the axial refractive index increases. The potential applications of the correspondence between geometrical ray optics and the operator representation of wave optics abound and the next steps will be to examine the lens paradox and to evaluate the PSF of the crystalline lens.

Acknowledgments

This work and the research of MT Flores-Arias were supported by the Spanish Ministerio de Educación y Ciencia under contract ESGHOPET/TIC 2003-03041. The GRIN Optics Group at USC is a NEMO/EU partner (Network of Excellence on Micro-Optics).

Appendix

We must prove that equation (27) is equal to equation (28). The first two terms of equation (27) can be expressed as [18]

$$P_b H_f = P_b + [H_f - 1]P_b = P_b - \frac{d_b}{n'_1} P_G P_b \quad (\text{A.1})$$

$$P_f \dot{H}_a = P_f + [\dot{H}_a - 1]P_f = P_f - \frac{d_b}{n'_1} P_G P_f. \quad (\text{A.2})$$

On the other hand, we can write [18]

$$\frac{d_f}{n_1} + \frac{d_b}{n'_1} = \frac{2 - H_f - \dot{H}_a}{P_G} \quad (\text{A.3})$$

and

$$\frac{d_f d_b}{n_1 n'_1} P_G = \frac{1 + \dot{H}_a H_f - \dot{H}_a - H_f}{P_G}. \quad (\text{A.4})$$

(A.3) and (A.4) show that

$$\frac{d_f}{n_1} + \frac{d_b}{n'_1} - \frac{d_f d_b}{n_1 n'_1} P_G = \frac{H_a}{n_e} \quad (\text{A.5})$$

where equations (19) and (20) have been used.

From equations (A.1), (A.2) and (A.5) it follows that

$$P_b H_f + P_f \dot{H}_a - \frac{H_a}{n_e} P_b P_f = P_b + P_f - \frac{d_b}{n'_1} P_G P_b - \frac{d_f}{n_1} P_G P_f - \left(\frac{d_f}{n_1} + \frac{d_b}{n'_1} \right) P_G P_f + \frac{d_f d_b}{n_1 n'_1} P_b P_f P_G. \quad (\text{A.6})$$

Therefore, equation (27) is equal to equation (28).

References

- [1] Luneburg R K 1964 *Mathematical Theory of Optics* (Berkeley, CA: University of California Press)
- [2] Stoler D 1981 *J. Opt. Soc. Am.* **71** 334–41
- [3] Nazarathy M and Shamir J 1982 *J. Opt. Soc. Am.* **72** 356–64
- [4] Nazarathy M and Shamir J 1982 *J. Opt. Soc. Am.* **72** 1398–408
- [5] Gómez-Reino C 1992 *Int. J. Optoelectron.* **7** 607–80
- [6] Abe S and Sheridan J T 1994 *J. Phys. A: Math. Gen.* **27** 4179–87
- [7] Abe S and Sheridan J T 1994 *Opt. Lett.* **19** 1801–3
- [8] Abe S and Sheridan J T 1994 *Opt. Commun.* **113** 385–8
- [9] Alieva T and Agulló-López F 1995 *Opt. Commun.* **114** 161–9
- [10] Shamir J and Cohen N 1995 *J. Opt. Soc. Am. A* **12** 2415–23
- [11] Nakao S, Ono T, Nagata R and Iwata K 1969 *Japan. J. Clin. Ophthalmol.* **23** 903–6
- [12] Blaker J W 1980 *J. Opt. Soc. Am.* **70** 220–3
- [13] Pierscionek B K and Chang D Y C 1989 *Optom. Vis. Sci.* **66** 822–9
- [14] Smith G, Pierscionek B K and Atchison D A 1991 *Ophthalmic Physiol. Opt.* **11** 359–69
- [15] Atchison D A and Smith G 1995 *Vis. Res.* **35** 2529–38
- [16] Smith G and Atchison D A 1997 *J. Opt. Soc. Am. A* **14** 2537–46
- [17] Pérez M V, Bao C, Flores-Arias M T, Rama M A and Gómez-Reino C 2003 *J. Opt. A: Pure Appl. Opt.* **5** S293–7
- [18] Gómez-Reino C, Pérez M V and Bao C 2002 *Gradient-Index Optics: Fundamentals and Applications* (Berlin: Springer)
- [19] Palma C and Bagini V 1997 *J. Opt. Soc. Am. A* **14** 1774–9
- [20] Freeman M H and Hull C C 2003 *Optics* 11th edn (London: Butterworth and Heinemann)
- [21] Gullstrans A 1924 *Helmholtz's Physiological Optics* (New York: Optical Society of America)
- [22] Cook C A, Koretz J F, Pfahnl A, Hyun J and Kaufman P L 1994 *Vis. Res.* **34** 2945–54
- [23] Koretz J F, Cook C A and Kaufman P L 2001 *J. Opt. Soc. Am. A* **18** 265–72